0.1 QCD

The search for subatomic structure has always played an important role in high energy particle physics experiments from Rutherford to the early SLAC electron experiments. We are now at the point where we are searching for substructure on at the TeV scale, or at distances of around 10^{-9}nm. As in the early SLAC electron scattering experiments where partons were observed inside nucleons, parton substructure can be observed once the energy of the probe is large enough such that their wavelengths become comparable to or smaller than the distance scales of the subpartons. In this case, we use partons from the protons and anti-protons as probes of each other in parton-parton scattering, and one can see deviations from QCD expectations by studying the energy transfered. Experimentally, one observes the E_T distribution of the jets in the final state for events which are believed to be purely QCD in nature. Any deviation from "pure QCD" which comes from parton substructure will show up in the jet E_T sprectrum as a "knee", raising the cross-section for high E_T.

The entire Run 1 data set based on an integrated luminosity of 92 pb$^-1$ with $\sqrt{s} =$ 1.8TeV is used in the analysis. Jets are defined using a fixed-cone algorithm to cluster energy with a cone radius of $\mathcal{R} = 0.7$ in $\eta - \phi$ space where η is the usual pseudorapidity variabled defined via $\eta \equiv -ln(tan\theta/2)$. The DØ measurements include the intervals $|\eta| \leq 0.5$ and $0.1 \leq |\eta| \leq 0.7$.

Events are first required to have a well measured event vertex within ± 50cm of the center of the detector. This requirement keeps $90 \pm 1\%$ of all jet triggered events.

Poorly measured events are further eliminated by rejecting events with large missing E_T to eliminate cosmic rays in time with the beam crossing $\not{E}_T < 30$ GeV or $0.3E_T^{MAX}$ (where E_T^{MAX} is from the highest E_T jet) whichever is larger. Quality cuts on the jets eliminate pathologically mismeasured jets as well as accelerator backgrounds by requiring

1. $0.5 <$EMF< 0.95
2. HCF> 0.1
3. CHF< 0.4

where EMF is the fraction of the total jet transverse energy deposited in the EM (inner) layers of the calorimeter, CHF ("course hadronic fraction") is the fraction of the jet transverse energy deposted in the course hadronic (outer) layers of the calorimeter, and HCF ("hot cell fraction") is the ratio of the energy in the second most energetic cell relative to the most energetic cell. Low EMF indicates noisy CH or FH cells, high EMF indicates noisy EM cells. High CHF is associated with main ring backgrounds, and low HCF indicates a fake jet by virtue of the fact that real jets have their hadronic energy spread out over several cells. The selection efficiencies have been measured as a function of jet E_T for the regions $|\eta| \leq 0.7$ to be $97 \pm 1\%$ below 250 GeV and $95 \pm 2\%$ at 400 GeV.

The transverse energy of the jet is measured by summing the transverse energy of all towers in the jet cone as discussed above:

$$E_{Tjet} = \sum_i E_{Ti}$$

where E_{Ti} is the transverse energy of tower i, derived from the measured energy E_i and tower coordinate θ_i using

$$E_{Ti} = E_i \sin \theta_i .$$

With the transverse jet energy in hand, corrections for underlying event, noise from uranium decay, parton showering outside the jet cone, detector uniformity, and detector hadronic response are made. For $|\eta| \leq 0.5$ the mean total correction for jet energies at $E_{Tmeasured} =$ 100GeV (400GeV) is 1.154 ± 0.017 (1.118 ± 0.023). Figure 1 shows the jet corrections and the uncertainties.

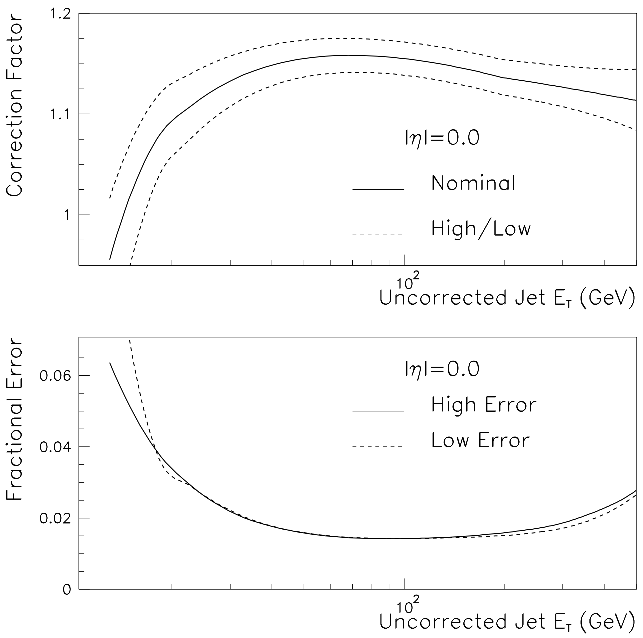

Figure 1: Jet E_T correction factor and uncertainty.

Distortions to the (steep) E_T spectrum due to the detector's jet energy resolution must be corrected in order to compare to theory. At any given jet E_T, the resolution is well described by a gaussian, measured using jet E_T balancing. The relative width of the gaussian σ_{E_T}/E_T is found to be $11 \pm 2\%$, $7.5 \pm 2\%$, and $4.5 \pm 2\%$ at 50, 100, and 400 GeV E_T respectively. Unsmearing is accomplished by generating a trial spectrum using the ansatz function

$$AE_T^{-B}(1 - \frac{2E_T}{\sqrt{s}})^C$$

and smearing with the above mentioned gaussian to generate a pseudo-measured jet E_T spectrum. The parameters A, B, and C are varied to obtain the best agreement with the measured jet E_T spectrum (after jet corrections). The optimal values for A, B, and C are then used to correct the measured jet E_T spectrum by taking the bin-by-bin ratio of the initial ansatz to the smeared ansatz. of the jet E_T along with the uncertainty.

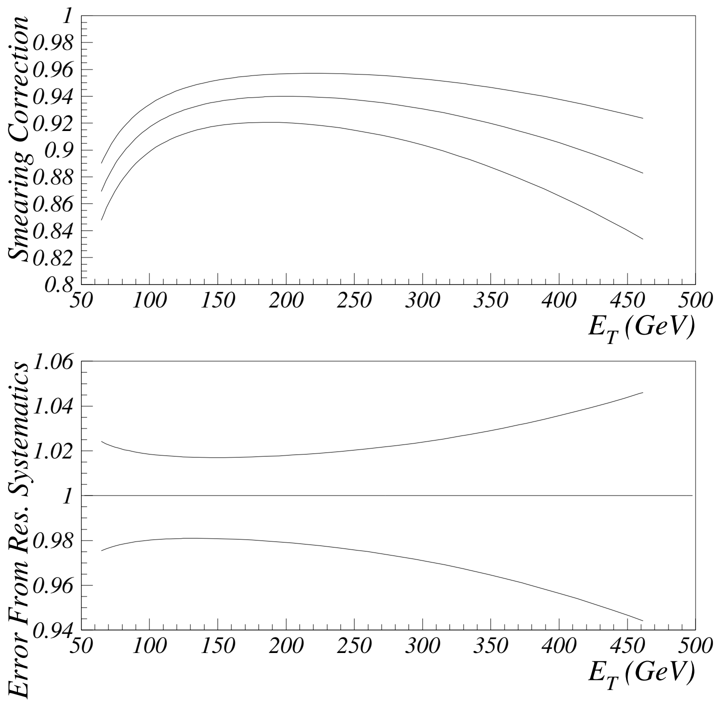

Figure 2: Jet E_T smearing correction factor and uncertainty.

In the central region $|\eta| \leq 0.5$, the DØ calorimeter is uniformly thick (7 or more interaction lengths with no gaps), and the energy resolution and calibration is well understood. Figure 3 shows the unsmeared cross-section for inclusive jets in the rapidity region $|\eta| \leq 0.5$ as a function of the jet E_T, averaged over the rapidity region and over each E_T bin, along with a theoretical prediction using the JETRAD[1] generator. The inputs to JETRAD are the renormalization scale μ ($\mu = 0.5E_T^{max}$ here), the parton clustering method (partons seperted by less than $\mathcal{R}_{sep} = 1.3\mathcal{R}$ were clustered if they were within $\mathcal{R}$ of their E_T-weighted centroid in $\eta - \phi$ space), and the parton distribution function (CTEQ3M[2] is used here). Variations in these inputs accounts for a 30% variation in the predicted cross-section. A 6.1% luminosity uncertainty is not shown in the plot.

The residuals (Data-Theory, normalized to Theory) are shown in figure 4 for the CTEQ3M pdf for the regions $|\eta| \leq 0.5$ and $0.1 \leq |\eta| \leq 0.7$. At low E_T, uncertainties in the luminosity and resultion dominate. At high E_T, uncertainties in the jet energy scale dominate. All 3 of these uncertainties are correlated over all E_T bins, resulting in an overall correlated uncertainty. Good agreement over 7 decades is clear from this plot, showing no indication of an excess relative to QCD in the data above 350 GeV. This analysis was published in 1999. [3].

subsubsectionKT Algorithm Studies

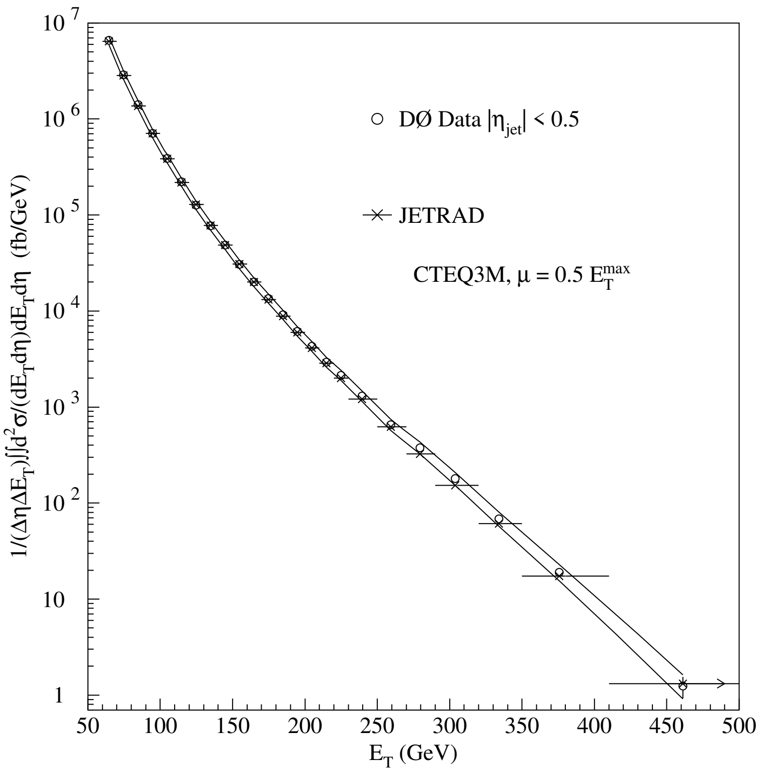

Figure 3: Jet E_T inclusive cross-section. Solid curves represent the 1-σ uncertainty band. Statistical errors are invisible.

During the calendar year 2000, a similar analysis is being readied using a different jet clustering technique as an alternative to the fixed cone algorithm. This variation implements a successive combination type of algorithm (called "KT"[4]) to reconstruct jets. This algorithm has been widely used at the DESY electron-proton and the CERN electron-positron colliders. The algorithm combines pairs of particles to make pseudo-particles for jet inclusion, and all particles are considered. Note that this algorithm has the advantages over the fixed cone clustering algorithm in that

- It can be implemented in the same manner at all levels of simulation (fixed order parton interaction, parton shower, final state hadrons, and calorimeter cells).
- Each particle/cell is assigned to one and only one jet eliminating the need for split/merge criteria.
- The absense of a cone boundary avoids out-of-cone showering losses, and thus corrections.

We expect to release results in the summer of 2000.

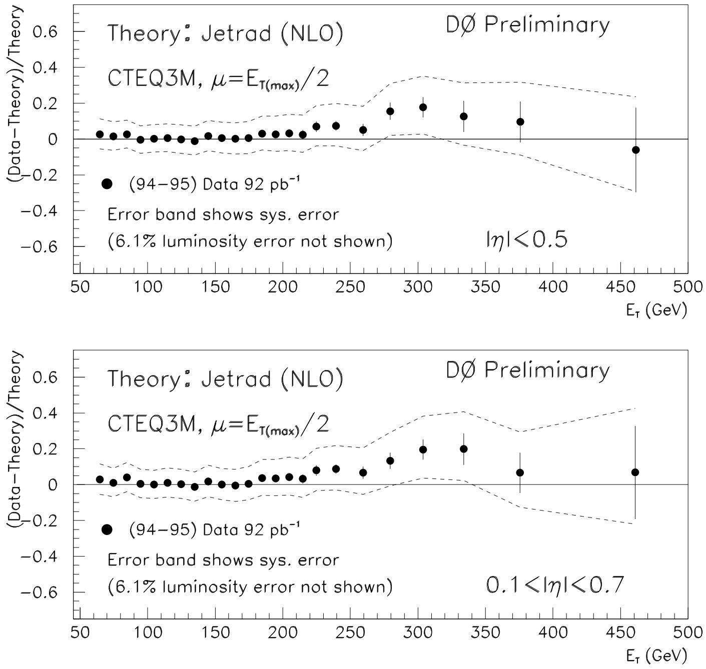

Figure 4: Differences between measured (after all corrections) and theory normalized to theory predictions. Bands represent total experimental uncertainty.

References

[1] W.T. Giele, E.W.N. Glover, and D.A. Kosower, Phys. Rev. Lett. **64**, 2121 (1990).

[2] H.L. Lai *et al.*, Phys. Rev. D **51**, 4763 (1995). H.L. Lai *et al.*, Phys. Rev. D **55**, 1280 (1997).

[3] B. Abbot *et al.* (DØ Collaboration), Phys. Rev. Lett. **82**, 2451 (1999).

[4] B. Abbot *et al.* (DØ Collaboration), Nucl. Instr. and Meth. **A** (1999) 352.